



Contents lists available at SciVerse ScienceDirect

Spectrochimica Acta Part A: Molecular and Biomolecular Spectroscopy

journal homepage: www.elsevier.com/locate/saa

Hybrid hard- and soft-modeling of spectrophotometric data for monitoring of ciprofloxacin and its main photodegradation products at different pH values

Mariela Razuc^a, Mariano Garrido^a, Yamile S. Caro^b, Carla M. Teglia^b, Héctor C. Goicoechea^b, Beatriz S. Fernández Band^{a,*}

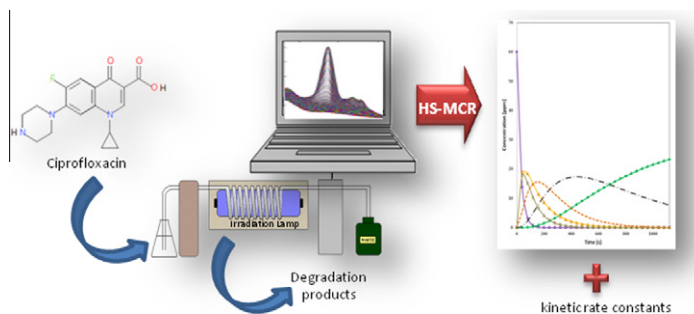
^aFIA Laboratory, Department of Chemistry, Universidad Nacional del Sur, INQUISUR (UNS-CONICET), Av. Alem 1253, Bahía Blanca (B8000CPB), Buenos Aires, Argentina

^bLaboratorio de Desarrollo Analítico y Quimiometría (LADAQ), Universidad Nacional del Litoral – CONICET, Ciudad Universitaria, Santa Fe (S3000ZAA), Argentina

HIGHLIGHTS

- ▶ Simple on-line UV method to study ciprofloxacin photodegradation is presented.
- ▶ MCR-ALS helps to propose a reliable kinetic pathway for the photodegradation.
- ▶ HS-MCR provides the kinetic profiles without using separation techniques.
- ▶ Kinetic rate constants for the photodegradation reaction are estimated.

GRAPHICAL ABSTRACT



ARTICLE INFO

Article history:

Received 16 August 2012

Received in revised form 7 December 2012

Accepted 31 December 2012

Available online 5 January 2013

Keywords:

Ciprofloxacin

Photodegradation

Multivariate curve resolution

Hard-soft modeling

ABSTRACT

A simple and fast on line spectrophotometric method combined with a hybrid hard-soft modeling multivariate curve resolution (HS-MCR) was proposed for the monitoring of photodegradation reaction of ciprofloxacin under UV radiation. The studied conditions attempt to emulate the effect of sunlight on these antibiotics that could be eventually present in the environment. The continuous flow system made it possible to study the ciprofloxacin degradation at different pH values almost at real time, avoiding errors that could arise from typical batch monitoring of the reaction. On the base of a concentration profiles obtained by previous pure soft-modeling approach, reaction pathways have been proposed for the parent compound and its photoproducts at different pH values. These kinetic models were used as a constraint in the HS-MCR analysis. The kinetic profiles and the corresponding pure response profile (UV-Vis spectra) of ciprofloxacin and its main degradation products were recovered after the application of HS-MCR analysis to the spectra recorded throughout the reaction. The observed behavior showed a good agreement with the photodegradation studies reported in the bibliography. Accordingly, the photodegradation reaction was studied by high performance liquid chromatography coupled with UV-Vis diode array detector (HPLC-DAD). The spectra recorded during the chromatographic analysis present a good correlation with the ones recovered by UV-Vis/HS-MCR method.

© 2013 Elsevier B.V. All rights reserved.

Introduction

Ciprofloxacin [1-cyclopropyl-6-fluoro-1,4-dihydro-4-oxo-7-(piperazin-1-yl)quinolone-3-carboxylic acid] is a synthetic fluoroquinolone derivative which has broad-spectrum activity against many pathogenic gram-negative and gram-positive bacteria, via inhibition of the DNA gyrase, responsible for the preservation of DNA [1,2]. Fluoroquinolones are widely used in the treatment of a variety of bacterial infections in human and veterinary medicine [3].

* Corresponding author. Tel.: +54 291 459 5100; fax: +54 291 459 5160.

E-mail address: usband@criba.edu.ar (Beatriz S. Fernández Band).

Ciprofloxacin was found in hospital effluents at concentration levels between 0.7 and 124.5 µg/L [4]. Unused therapeutic drugs

are sometimes disposed into the sewage system. If the drugs are not degraded or eliminated during sewage treatment, in soil or in other environmental compartments, they will reach surface water, ground water and, potentially, drinking water. Non-metabolized antibiotic substances often pass into the aquatic environment in wastewater. Antibiotics used in veterinary medicine, or as growth promoters, are excreted by the animals and wind up in the feces, which is afterward used as agricultural fertilizer. Thus, the antibiotics leak gradually through the soil and enter in the ground water [5]. Among other problems, antibiotics cause resistance in several bacteria [4,6]. The correlation between fluoroquinolone consumption in ambulatory care and resistance increase was already demonstrated [7]. Moreover, it is not clear if degradation of the main products could give rise to other minor compounds with undesirable or toxic effects. Therefore, it becomes necessary to understand how these antibiotics and/or their corresponding secondary products behave in the environment under different conditions (such as pH, UV radiation, temperature) with a view to developing feasible methods to determine the actual concentration of these contaminants and/or to remediate the polluted environment.

Ciprofloxacin undergoes photodegradation in aqueous solutions after irradiation with a high-pressure mercury lamp or after exposure to daylight [8–10]. Photodegradation can be influenced by pH since fluoroquinolones are amphoteric substrates. Thus, the species present in solution depend on the pH and, consequently, the photochemistry is expected to be pH-dependent [11]. The structural elucidation of ciprofloxacin photodegradation products in aqueous solutions at different pH values has been the subject of numerous investigations [2,11–14].

Reaction monitoring has been traditionally studied by taking aliquots of the reacting mixture and, afterwards, analyzing them by separation techniques. Thus, monitoring of ciprofloxacin photodegradation reactions is normally performed by liquid chromatography [2,12,14–16] and, to a lesser extent, by gas chromatography [17] and capillary electrophoresis [16]. However, taking representative aliquots of the reacting mixture could be difficult, or sometimes the reacting systems could be unstable. Moreover, the reaction may continue in the lapse of time between the sampling and the further analysis. These problems could be overcome carrying out *in situ* spectroscopic measurements.

Spectroscopic monitoring could give important information about the chemical reaction. Typically, the spectral information is used in a univariate mode, i.e. some spectral bands are assigned to the studied compounds in the reacting mixture. However, often there is spectral overlap and lack of selectivity in the spectral bands. In these conditions, it is barely possible to follow the kinetic profiles only for few of the species that take part in the reaction. In this sense, a multivariate treatment of spectral data could be helpful to find out more about the process that is being carried out. When the so-called multivariate curve resolution methods (soft-modeling methods) are applied to bilinear spectroscopic data obtained from the monitoring of a chemical reaction, the concentration profiles of each species involved in the reaction and the corresponding pure spectra can be estimated. This procedure is performed without explicitly using the underlying chemical model linked to the reaction process [18]. Several studies in the literature have used these methods to analyze photochemical reactions [19–22]. Also, a comprehensive review including these techniques (among other chemometric tools) has been published [23]. In addition, the concentration profiles obtained by multivariate curve resolution methods can be used to design a suitable reaction model and to support the model chosen for a hypothetical reaction under study [24]. However, the profiles obtained by these soft-modeling methods are affected by ambiguities [25,26] that impede obtaining unique solutions. One way to minimize the ambiguity associated to soft-modeling solutions is to compel the system to fulfill a kinetic model, which acts as a constraint through-

out the resolution process [27–30]. This 'hard-modeling' step involves the non-linear least-squares (or similar) fitting of the parameters of a chemical model that describes the data. The fitting is carried out on the concentration profiles without taking into account the spectral contributions (linear parameters) [31]. As a result, new kinetic profiles are obtained and the rate constants (non-linear parameters) are additionally acquired [27]. In the current study, 'hard and soft-modeling' multivariate curve resolution (HS-MCR) is applied [24,27]. This approach has the advantages of both pure soft- and pure hard-modeling [24].

The current article is focused on studying the changes that the ciprofloxacin and its principal degradation products could suffer under UV-radiation at different pH values. The studied conditions attempt to emulate the effect of sunlight on these antibiotics that could be eventually present in the environment. Photodegradation reaction was carried out in a flow system, so the UV-Vis monitoring was performed in a continuous way (i.e. no aliquots need to be taken off from the reacting mixture), almost at real time. In this way, the errors arising from the batch monitoring could be avoided. The UV-Vis spectra recorded throughout the time were arranged in matrices and subsequently analyzed using HS-MCR. The combination of UV-Vis monitoring and HS-MCR made it possible to study the kinetic behavior of the photodegradation reaction without using separation techniques, with the consequent saving of time. Moreover, the kinetic rate constants associated to the degradation process could be obtained as additional information.

Materials and methods

Reagents and solutions

Analytical reagent-grade chemicals and ultra pure deionized water ($18.3 \mu\text{cm}^{-1}$, Barnstead, Dubuque, USA) was used. Ciprofloxacin (BioChemika Fluka) stock solution of 1000 mg L^{-1} was prepared with ultra pure water. Britton Robinson buffer solutions (pHs 5.0, 7.0 and 9.0) were prepared by mixing appropriate volumes of 0.04 mol L^{-1} of acid solutions: acetic acid (Mallinckrodt), phosphoric acid (Mallinckrodt) and boric acid (Sigma) and a 0.2 mol L^{-1} NaOH solution (Anedra). Ciprofloxacin working solution of 60 and 10 mg L^{-1} were prepared by appropriate dilution of ciprofloxacin stock solution with the corresponding buffer solutions.

Apparatus

All the flow system components were made of PTFE (0.5 mm i.d.). Photoreactor (12 m in length) was helically arranged around a low mercury UV lamp with a power of 15 W (Phillips). This typical germicide lamp has a maximum emission line at 254 nm. A diode array spectrophotometer Agilent 8453 equipped with a Hellma 178-712-QS flow cell with an inner volume of $8 \mu\text{L}$ and 10 mm light path, was used. Fluids in the flow system were pumped with a Gilson Minipuls 3 peristaltic pump.

The chromatographic analysis was carried out in a modular Agilent 1100 Series instrument (Agilent Technologies, Waldbronn, Germany) with UV diode array detector (DAD). The separation was performed in a 5 μm Zorbax Eclipse XDB-C18 column ($4.6 \times 150 \text{ mm}$). The mobile phase was acetonitrile-phosphoric acid (20 mmol L^{-1} , pH 2.3) 15:85 v/v + 2.5 mmol L^{-1} hexane-sulfonic acid sodium salt (Na-HSA) at a flow-rate of 1.5 mL min^{-1} [12]. All measurements were done at room temperature.

Experimental procedure

The ciprofloxacin solution was pumped into the single channel flow system (Fig. 1) to fill the photoreactor (12 m). Then, the flow

rate was fixed at 0.1 mL min^{-1} and the UV-lamp was switched on (initial time, t_0). In this way, we assume that the first portion of ciprofloxacin leaving the reactor corresponds to $t_0 = 0 \text{ s}$ of photodegradation time, whereas the last portion of ciprofloxacin solution reaching the detector has a maximum residence time into the photoreactor of 18.8 min. The spectra were recorded from 210 to 400 nm ($\Delta\lambda = 2 \text{ nm}$), every 4 s, exported and converted into MATLAB® binary files [32]. The experimental data were arranged in matrices whose rows were the recorded spectra for each reaction time and whose columns were the wavelengths. The following matrices were thus obtained: \mathbf{A}_1 (282×96), \mathbf{A}_2 (282×96), and \mathbf{A}_3 (282×96) corresponding to the degradation of ciprofloxacin solutions of 60 mg L^{-1} at pHs 5.0, 7.0 and 9.0, respectively. Also matrices \mathbf{B}_1 (150×96), \mathbf{B}_2 (150×96), and \mathbf{B}_3 (150×96) were obtained and they correspond to the spectra recorded throughout the degradation of ciprofloxacin solutions of 10 mg L^{-1} at the same pH values. Augmented data matrices \mathbf{D}_1 (432×96), \mathbf{D}_2 (432×96), and \mathbf{D}_3 (432×96) were arranged with the individual \mathbf{A}_i and \mathbf{B}_i matrices corresponding to each pH value (e.g. \mathbf{D}_1 was constructed with \mathbf{A}_1 and \mathbf{B}_1 matrices).

For the chromatographic analysis, the photodegradation reaction was separately conducted starting with ciprofloxacin at a concentration level of 60 mg L^{-1} . Aliquots of the reacting mixture were withdrawing at times of 0, 64, 152, 400 and 800 s. After appropriate dilution the samples were injected into the chromatographic system.

Data analysis

Multivariate curve resolution-alternating least squares

Multivariate curve resolution optimized by alternating least squares makes it possible to obtain a bilinear decomposition of the experimental data matrix, based on the multiwavelength extension of Beer's law, as follows:

$$\mathbf{D} = \mathbf{CS}^T + \mathbf{E} \quad (1)$$

where \mathbf{D} is the experimental data matrix, \mathbf{C} is the matrix describing the changes in the concentration of the species present in the system under study, \mathbf{S}^T is the matrix containing the response profile of these species (spectral profiles), and \mathbf{E} is the residual matrix with the data variance unexplained by \mathbf{CS}^T [33,34]. This decomposition involves the following steps:

- (1) The determination of the number of components that cause the variability observed in the experimental data matrix \mathbf{D} (chemical rank). In the current study, the rank of the individual and the augmented data matrices was analyzed with singular value decomposition (SVD) [35] and Evolving Factor Analysis [36]. Considering that the chemical components made a much larger contribution to the data variance than noise and experimental error, it was enough to estimate the number of factors by simple inspecting the tables of singular values. The rank deficiency problems of the experimental data matrices was solved by means of column-wise matrix augmentation [37,38].
- (2) Construction of the initial estimate: In this study, the initial estimates of the pure spectra were obtained by using the SIMPLISMA algorithm, a technique based on selecting of the 'purest' variables [39]. SIMPLISMA was applied to each augmented matrix \mathbf{D}_i to search for spectral estimates of the different components.
- (3) Optimization by alternating least squares (ALS): The applied constraints were the following:
 - (a) The values of the spectra of each component must be non-negative.
 - (b) The values of the concentration profiles as a function of time must be non-negative.
 - (c) When multiple matrices are simultaneously analyzed by column-wise matrix augmentation, additional conditions are fulfilled: the pure spectra of common components in the different experiments (matrices) are equal and there is correspondence of common components among experiments.

Hard-soft-modeling multivariate curve resolution (HS-MCR)

A function consisting of the differential equations representing the variation in concentration of the species over time was constructed in accordance with the kinetic model proposed (see Section 3.3). An ordinary differential equation solver (ODE23) that comes with MATLAB® was used to solve the differential equations [32,40]. It required some initial information: the starting concentrations for each of the species considered in the model, a vector specifying the various time points for the reaction times and an initial estimate of the kinetic rate constants. A multi-parameter minimum search procedure, based on the Nelder–Mead algorithm [41] found the rate constants that provided the best fit between the profiles obtained from the kinetic model and the resolved concentration profiles during each iteration of the ALS optimization.

Results and discussion

Selecting of the number of components

The correct application of multivariate curve resolution strongly depends on the appropriate selection of the number of components or factors. Resolution of the system is possible if the rank of the data matrix (chemical rank) is assumed to be equal to the number of absorbing species when no other contributions, such as instrumental noise, are present. When the number of significant contributions to the data variance is lower than the real number of chemical species present in the system the system is rank-deficient. The selection of the appropriate number of components was carried out by Singular Value Decomposition (SVD) and assisted also by Evolving Factor Analysis, which corroborates the number of components given by SVD. Table 1 shows the first seven singular values associated to the singular value decomposition for the individual data matrices \mathbf{A}_1 , \mathbf{A}_2 and \mathbf{A}_3 and the corresponding augmented matrices \mathbf{D}_1 , \mathbf{D}_2 and \mathbf{D}_3 for the experiences at pHs 5.0, 7.0 and 9.0, respectively. The rank analysis of the individual

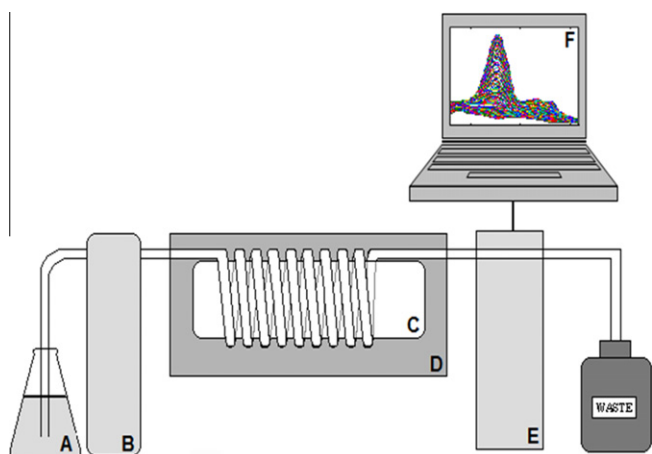


Fig. 1. Schematic representation of the flow photodegradation system for ciprofloxacin. Ciprofloxacin solution (A), peristaltic pump (B), UV lamp (C), protector box (D), spectrophotometer (E), personal computer (F).

Table 1
Singular values corresponding to the SVD of the studied matrices.

pH 5		pH 7		pH 9	
D ₁	A ₁	D ₂	A ₂	D ₃	A ₃
46.6	31.9	38.4	27.9	31.3	23.4
8.5	6.6	5.5	3.8	5.2	3.5
1.1	0.8	1.1	0.8	1.2	0.9
0.3	0.1	0.6	0.3	0.6	0.4
0.2	0.1	0.3	0.1	0.3	0.1
0.1	<0.1	0.1	<0.1	0.2	<0.1
<0.1	<0.1	<0.1	<0.1	<0.1	<0.1

data matrices shows a number of five components for all the experiences at pHs 5.0, 7.0 and 9.0. However, if augmented matrix were analyzed, the rank increases by one unit for all the matrices. One explanation for this fact is that, when the systems analyzed come from processes in evolution, the data sets are often rank-deficient. In the case of reacting mixtures, a rank deficiency can appear in concentration matrix **C** for several reasons. The concentration profiles of the absorbing species may be not linearly independent because of the underlying reaction network [42]. In these cases, the rank deficiency could be overcome by column-wise matrix augmentation [36,37]. This rank augmentation by matrix augmentation has been obtained by joining various matrices from various process runs that started with different initial concentration of ciprofloxacin. For each additional matrix, the rank of the augmented matrix can increase by one unit until the maximum value is equal to the total number of absorbing species [36]. In the current data set no further rank increase was obtained when more than two individual matrices were included in the augmented one. So, the rank for the augmented matrices was six for **D**₁, **D**₂ and **D**₃. Later, the MCR-ALS analysis was carried out taking into account one component more than the number of components suggested by SVD. The obtained quality parameters (i.e. lack of fit and % of explained variance), the excessive number of iterations and divergence in the optimization process indicated that the model was overfitted under these conditions. So, the number of components obtained by SVD was used in subsequent analysis.

Soft-modeling and proposed kinetic models

The kinetic model for the system was postulated on the basis of the shape of the concentration profiles obtained after the soft-

modeling approach had been applied and taking into account the previous knowledge available about the system. The soft-modeling was carried out by applying MCR-ALS under the constraint of non-negativity and no kinetic information was required. As an example, Fig. 2 shows the concentration profiles obtained after the application of MCR-ALS to the spectral data corresponding to the monitoring of the experiments conducted at pHs 5, 7 and 9, but only for the reaction with ciprofloxacin initial concentration of 60 mg L⁻¹.

Several kinetics mechanisms have been proposed in the literature for the photodegradation of ciprofloxacin, depending on the reaction medium (pH, type of buffer, etc.). It is known that polynuclear (hetero) aromatics are not expected to photo rearrange [43] or to abstract hydrogen atoms [44]. Thus, the reactions taking place after photoexcitation are due to processes involving substituents. The principal reactions include defluorination, decarboxylation, oxidation of the side-chain amino substituent at C7 and reaction with reactive oxygen species [45].

It is important to note that, in the current study, the photodegradation was carried out in air-equilibrated solutions. In these conditions and in the presence of phosphate anion, defluorination is less significant than when the photodegradation is performed in aqueous medium and in Ar-flushed solution [11,13,46].

Also, a regression of $\ln(C/C_0)$ vs. photodegradation reaction time was investigated for ciprofloxacin. In the C/C_0 ratio, the concentration C of ciprofloxacin was obtained for each degradation time from the MCR-ALS profiles, and C_0 was the initial concentration of ciprofloxacin. A straight line was obtained in all cases (for all the pHs studied and for the different initial concentrations of ciprofloxacin), which indicates that ciprofloxacin degradation follows a first order kinetic (see Table 2).

On the base of these considerations we proposed different reaction pathways for the ciprofloxacin photodegradation, in accordance with the data reported in the literature and the used experimental conditions. Scheme 1 shows the photodegradation pathway proposed for the reaction at pH 5.0. In the scheme, ciprofloxacin degrades into three sub products. The compound 'a' results from defluorination and subsequent oxidation of the piperazine ring of the ciprofloxacin. Concretely, the phosphate radical abstracts a hydrogen atom from the piperazine ring, and the radical undergoes ring cleavage and H₂O addition to finally give this compound [11,13]. In acidic conditions, the piperazine ring is also oxidatively degraded, without losing of fluorine to give compound 'c' [8,13]. Likewise, other possible way is an earlier

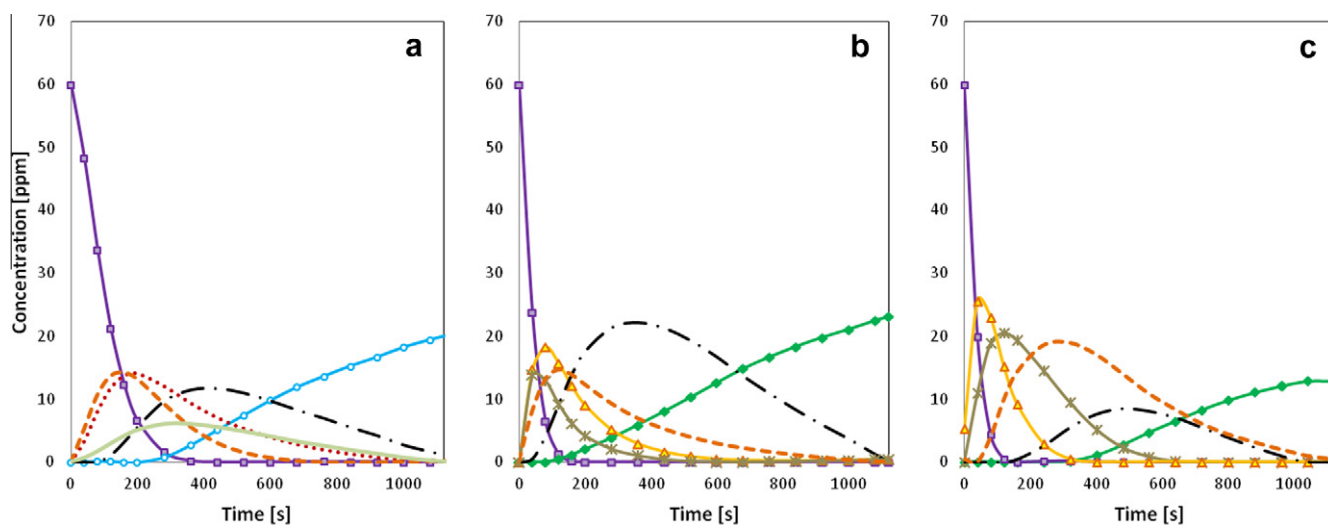


Fig. 2. Concentration profiles of ciprofloxacin (60 mg L⁻¹) and its main degradation products as a function of lighting time recovered by MCR-ALS: (a) pH 5.0, (b) pH 7.0 and (c) pH 9.0. Ciprofloxacin (■), compound 'a' (dashed line), compound 'b' (dotted line), compound 'c' (solid line), compound 'd' (dash-dotted line), compound 'e' (○), compound 'f' (▲), compound 'g' (✱) and compound 'h' (◆).

Table 2

Straight line regressions corresponding to $\ln(C/C_0)$ vs. photodegradation reaction time conducted for the ciprofloxacin photodegradation at different pH values. C values were recovered from MCR-ALS analysis.

Experiment	Straight line regression	R^2
pH 5	$y = -0.0105x + 0.1757$	0.991
pH 7	$y = -0.0336x + 0.3139$	0.991
pH 9	$y = -0.0263x + 0.0173$	0.998

oxidation product 'b' which subsequently gives compound 'c' in a more deep stage of the oxidization reaction [16]. In the course of the photodegradation, compound 'c' give rise the compound 'd' via reductive defluorination [14]. The same compound is obtained by a deep-seated degradation of the piperazine moiety to a [2-(formylamino)ethyl]methylamino group [13]. In acidic solutions, compound 'c' undergoes degradation of the piperazine side chain until this latter is reduced to an amino group (compound 'e') [13,45].

Scheme 2 shows the kinetic pathway proposed for the photodegradation reaction at pHs 7.0 and 9.0. In the scheme, ciprofloxacin degrades into two sub products: The first one is compound 'g', which arose from reductive dehalogenation of ciprofloxacin [47]. The second one is compound 'f' for which the addition of water to the fluoroquinolone triplet was proposed, leading to the photo-substitution of the fluorine atom by a hydroxyl group [41]. This product is generated mainly under alkaline conditions and with an air-saturated solution [11,45]. The oxidation of the piperazine ring of compound 'g' gives rise to compound 'a', which originates compound 'd' after reduction. Compound 'd' shows the presence of electron donating substituents in C7 which, under irradiation, facilitate the losing of carboxylic group (compound 'h') [48]. It is

important to note that fluorinated species are expected at very low concentration levels when photodegradation is conducted at neutral or alkaline media [11,13].

Application of HS-MCR

On the base of the kinetic pathways depicted in Schemes 1 and 2, the following differential equations were proposed for the photodegradation conducted at pH 5:

$$d[\text{Cipro}]/dt = -k_1[\text{Cipro}] - k_2[\text{Cipro}] - k_3[\text{Cipro}] \quad (2)$$

$$d[a]/dt = k_1[\text{Cipro}] - k_5[a] \quad (3)$$

$$d[b]/dt = k_3[\text{Cipro}] - k_4[b] \quad (4)$$

$$d[c]/dt = k_2[\text{Cipro}] + k_4[b] - k_6[c] - k_7[c] \quad (5)$$

$$d[d]/dt = k_5[a] + k_6[c] - k_8[d] \quad (6)$$

$$d[e]/dt = k_7[c] - k_9[e] \quad (7)$$

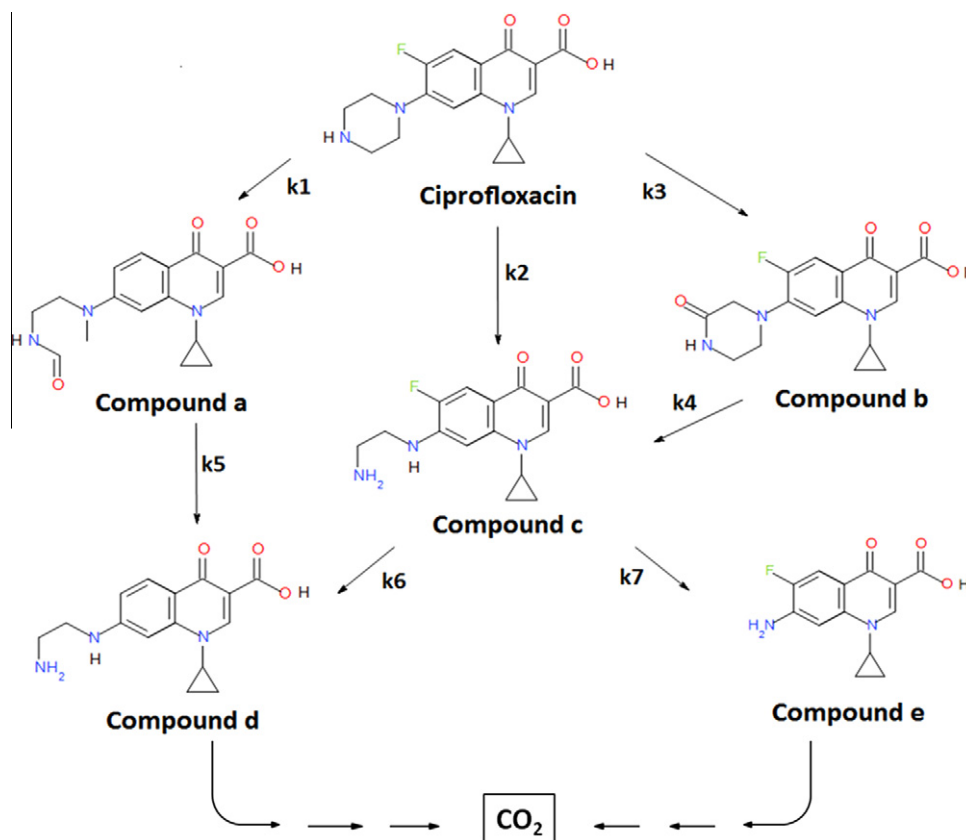
On the other hand, the differential equations proposed for Scheme 2 (i.e. the photodegradation conducted at pHs 7 and 9) were:

$$d[\text{Cipro}]/dt = -k_1[\text{Cipro}] - k_2[\text{Cipro}] \quad (8)$$

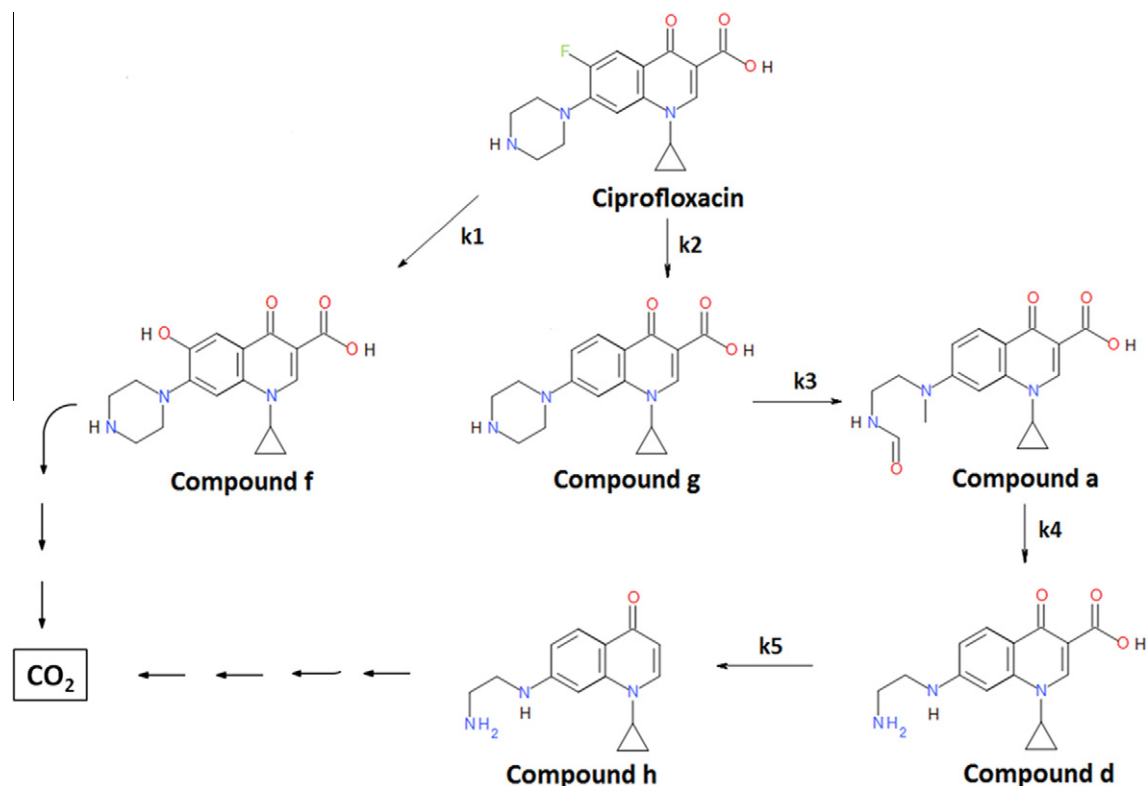
$$d[f]/dt = k_1[\text{Cipro}] - k_6[f] \quad (9)$$

$$d[g]/dt = k_2[\text{Cipro}] - k_3[g] \quad (10)$$

$$d[a]/dt = k_3[g] - k_4[a] \quad (11)$$



Scheme 1. Photodegradation pathway proposed for the reaction at pH 5.0.



Scheme 2. Photodegradation pathway proposed for the reaction at pH 7.0 and pH 9.0.

$$d[d]/dt = k_4[a] - k_5[d] \quad (12)$$

$$d[h]/dt = k_5[d] - k_7[h] \quad (13)$$

The HS-MCR algorithm was applied to the data set as mentioned in Section 2.4 and the concentration profiles were fitted to the proposed kinetic model (Eqs. (2)–(7) for the photodegradation at pH 5 and Eqs. (8)–(13) for the photodegradation at pHs 7 and 9).

Fig. 3a–c shows the concentration profiles recovered by HS-MCR for the photodegradation process of ciprofloxacin at pH values of 5.0, 7.0 and 9.0, respectively for the two different initial concentration. The values of the quality parameters corresponding to the ALS adjustment of the experiences at pHs 5.0, 7.0 and 9.0, respectively, were the following: 2.7%, 3.5% and 6.5% for the lack of fit and 99.92%, 99.88% and 99.58% for the explained variance. These quality parameters make it possible to suppose that, in a global manner, the proposed pathways were correct. It is important to note that there is serious spectral overlap in the recovered spectral profiles (Fig. 4), so the values of lack of fit could be considered very satisfactory. The recovered concentration profiles (Fig. 3) were similar in shape to the obtained ones in the soft modeling results (Fig. 2).

Table 3 shows the values of the photodegradation rate constants obtained by HS-MCR for the experiments carried out at different pH values. In order to compare the photodegradation rate of ciprofloxacin recovered by HS-MCR with the reported ones in the bibliography, a global rate constant should be taken into account. The ciprofloxacin photodegradation could be considered a competitive first order reaction, in which the parent compound give rise to two or three photoproducts. The corresponding global reaction rate constant could be expressed as the sum of the constants of the individual competing reactions [49].

So, the photodegradation rates constants of ciprofloxacin obtained for pHs 5.0, 7.0 and 9.0 were $0.0153 \text{ s}^{-1} (k_1 + k_2 + k_3)$,

$0.0318 \text{ s}^{-1} (k_1 + k_2)$, $0.0248 \text{ s}^{-1} (k_1 + k_2 + k_3)$ respectively. Despite the fact that the experiments reported in the bibliography have been conducted under different conditions (presence or absence of buffer, type of buffer, intensity of UV lamp, etc.) the rate constants obtained by HS-MCR are not quite different from the ones reported in the literature (0.0153 s^{-1} reported by Vasconcelos et al. [14] and 0.0041 s^{-1} reported by Fernández et al. [48]).

From the constant rate values and the kinetic profiles recovered by HS-MCR, the photodegradation of ciprofloxacin seems to be pH-dependent. Photodegradation is slow at pH 5.0, considerably accelerated at pH 7 which is very close to the iso-electric point of ciprofloxacin and slower at alkaline pH values. This fact is also in agreement with the literature [11,14]. The half-live times ($t_{1/2}$) of ciprofloxacin, calculated on the base of HS-MCR concentration profiles, were 45, 18 and 28 s at pHs 5.0, 7.0 and 9.0, respectively.

The recovered rate constants also evidence the influence of the concentration of phosphate ions in the reacting mixture. Fig. 3b and c shows that the photodegradation profiles of compounds involved in the formation of compound 'h' have greater importance at pH 7 than at pH 9. The rate constant values shown in Table 3 also show that, whereas the formation of compound 'f' is almost the same at both experiments, constants k_2 – k_5 are higher at pH 7. Mella et al. [13] reported that the ratio [compound 'a']/[compound 'f'] (see Scheme 2) linearly depends on the concentration of phosphate ions. In our experiments, the Britton–Robinson buffer used to prepare the ciprofloxacin solutions contains higher concentration of phosphate at pH 7 than at pH 9. Thus, the concentration of compound 'a' (i.e. the compounds that initiate the reaction chain that ends in the formation of compound 'h') is higher at pH 7 and the related rate constants are greater in these conditions than at pH 9.

Jointly with the concentration profiles, a set of spectra were recovered by HS-MCR for each experiment (at different pH values).

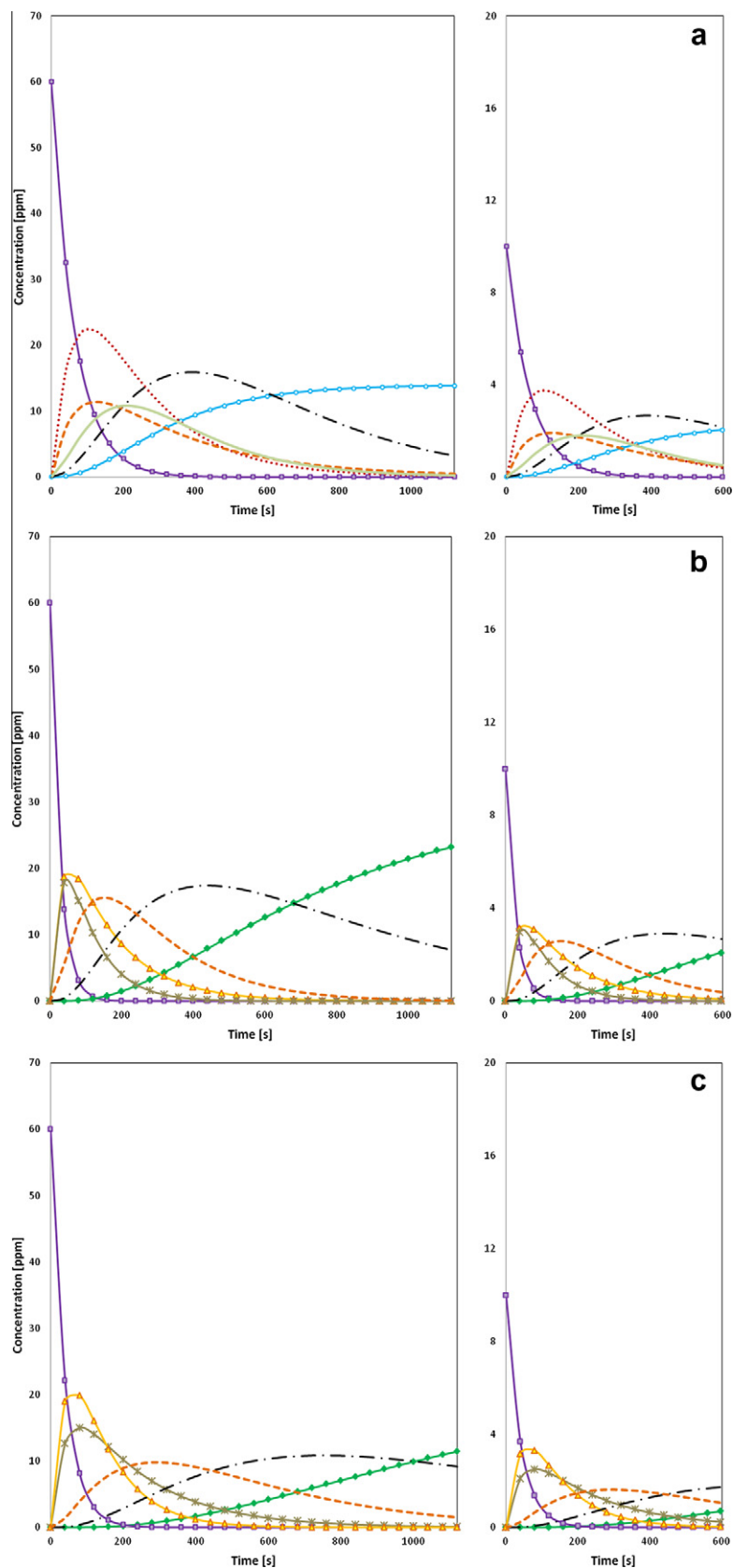


Fig. 3. Concentration profiles of ciprofloxacin (60 mg L^{-1} and 10 mg L^{-1}) and its main degradation products as a function of lighting time recovered by HS-MCR: (a) pH 5.0, (b) pH 7.0 and (c) pH 9.0. Ciprofloxacin (\square), compound 'a' (dashed line), compound 'b' (dotted line), compound 'c' (solid line), compound 'd' (dash-dotted line), compound 'e' (\circ), compound 'f' (\triangle), compound 'g' ($*$) and compound 'h' (\blacklozenge).

As an example, a set of spectra associated to all the species found at whichever of the studied pH values, is shown in Fig. 4. Spectra

obtained for the same compounds at different pH values are quite similar. However, there are some spectral regions (210–230 nm

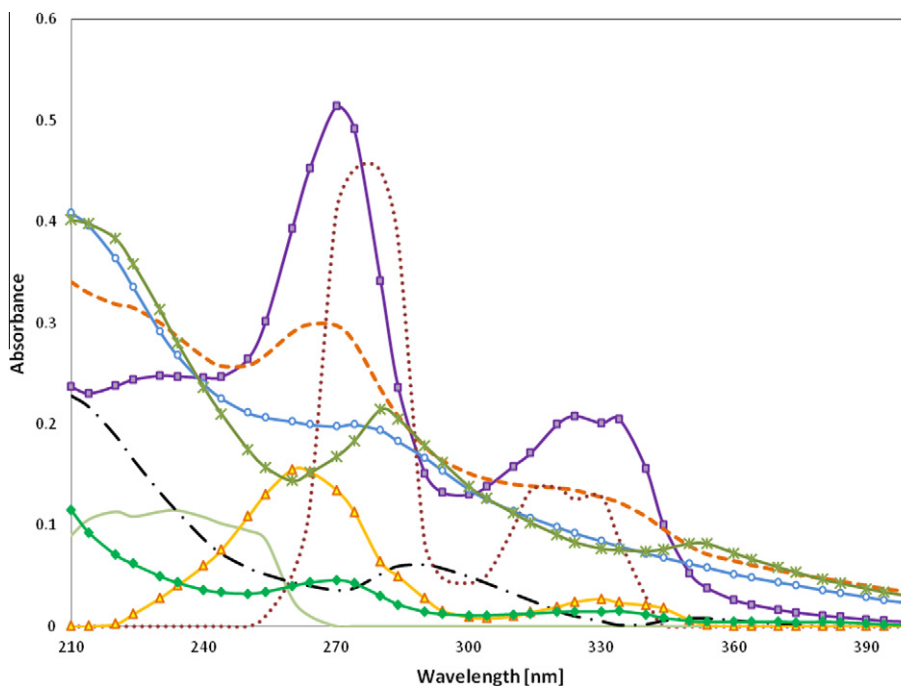


Fig. 4. Recovered pure spectra of ciprofloxacin (■) and its main degradation products by HS-MCR: compound 'a' (dashed line), compound 'b' (dotted line), compound 'c' (solid line), compound 'd' (dash-dotted line), compound 'e' (○), compound 'f' (▲), compound 'g' (✱) and compound 'h' (◆).

Table 3

Kinetic rate constants obtained by HS-MCR for the experiments conducted at different pH.

pH	k_1	k_2	k_3	k_4	k_5	k_6	k_7
pH 5	0.0045	0.0006	0.0102	0.0055	0.0035	0.006	0.0029
pH 7	0.0153	0.0165	0.0128	0.0059	0.0019	–	–
pH 9	0.0156	0.0093	0.005	0.0033	0.0013	–	–

and 320–350 nm) at which certain differences appear at different pH values. This fact hinders the possibility of performing a simultaneous analysis of the experiments conducted at different pH values, because of the lack of bilinearity in the data set.

Also, a chromatographic analysis was performed for the experiments at different pHs with ciprofloxacin initial concentration of 60 mg L⁻¹. As was mentioned before, samples were withdrawing at different reaction times (0, 64, 152, 400 and 800 s). This selection was carried out considering those reaction times more representative of the proposed reaction pathway, as indicated by the

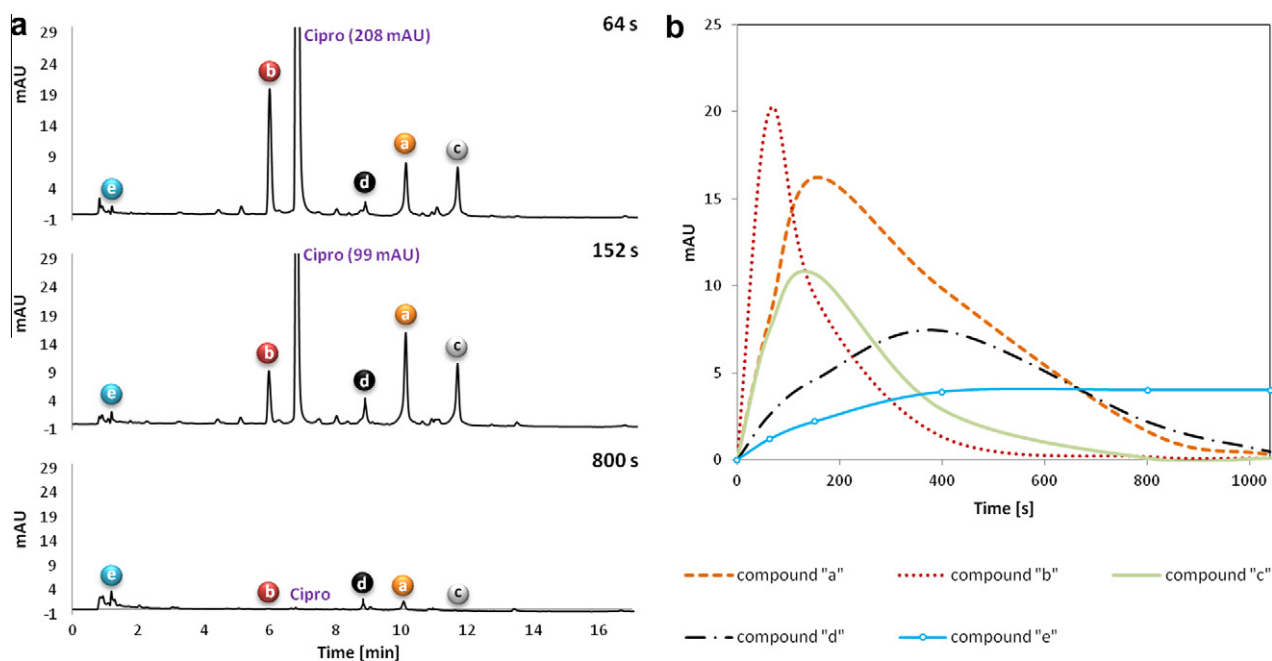


Fig. 5. (a) chromatograms obtained by HPLC/DAD for the photodegradation reacting mixture withdrawing at 64, 152 and 800s. (b) Evolution of the UV signal of chromatographic peaks throughout the photodegradation time.

concentration profiles obtained from the HS-MCR analysis. Fig. 5a shows, as an example, the more representative chromatograms (reaction times: 64 s, 152 s and 800 s) for the experiment conducted at pH 5. Also, the signals obtained for the chromatographic peaks corresponding to each compound were graphed vs. the photodegradation time (Fig. 5b). As can be seen, the evolution of the signals throughout the time shows a great similarity with respect to the concentration profiles obtained by HS-MCR. The identification of each peak with the corresponding photoproduct was carried out by inspecting Fig. 5b) and the correlation coefficients between the spectra recovered by HS-MCR and the ones obtained by HPLC-DAD.

Spectra recovered by MCR-ALS and HS-MCR were compared with the ones obtained by HPLC-DAD. In a global manner, there is a good correlation between them. For the experiment carried out at pH 5, the values of the correlation coefficients ranged between 0.82 and 0.99 for MCR-ALS spectra and between 0.85 and 0.98 for HS-MCR spectra. The low values were associated with compound a. When the experiment at pH 7 was analyzed, the correlation coefficients were within 0.84 and 0.96 for MCR-ALS and within 0.85 and 0.96 for HS-MCR. In this case, the lower correlation was observed for compound f. Finally, for the experiment at pH 9, the correlation coefficients ranged from 0.84 to 0.91 for MCR-ALS and from 0.83 and 0.92 for HS-MCR. The lower correlation was obtained for compound g.

Conclusions

The proposed continuous flow system, in combination with spectrophotometric monitoring and HS-MCR analysis, made it possible to study the photodegradation behavior of the ciprofloxacin and some of its main absorbent degradation products under UV radiation, and also to estimate the corresponding kinetic rate constants. The continuous monitoring avoids the manipulation of the reacting mixture and allows the measurements to be performed almost in real time. A prior application of MCR-ALS gave a set of concentration profiles for ciprofloxacin and several photoproducts without using separation techniques. The obtained concentration profiles provided valuable information to propose kinetic pathways for the photodegradation reactions carried out under different pH values. These kinetic models were imposed as a constraint in the ALS iteration process (HS-MCR). The behavior observed for the parent compound and the principal degradation products are in close agreement with other ciprofloxacin degradation studies found in the bibliography, and the kinetic rate constants obtained are comparable to the ones reported for similar degradation conditions. The proposed method represents a useful tool to study, in a rapid and reliable way, a reacting system when not much information about it is available.

Acknowledgements

The authors would like to acknowledge to Consejo Nacional de Investigaciones Científicas y Técnicas (CONICET). Mariela Razuc thanks the doctoral fellowship granted by Agencia de Promoción Científica y Tecnológica. Also, B.S. Fernández Band, M. Garrido and M. Razuc gratefully acknowledge the financial support of Universidad Nacional del Sur.

References

- [1] M. LeBel, *Pharmacotherapy* 8 (1988) 3–33.
- [2] E. Turiel, G. Bordin, A.R. Rodríguez, *J. Environ. Monit.* 7 (2005) 189–195.
- [3] L. Piddock, *Br. Med. J.* 317 (1998) 1029–1030.
- [4] A. Hartmann, E.M. Golet, S. Gartsler, A.C. Alder, T. Koller, R.M. Widmer, *Arch. Environ. Contam. Toxicol.* 36 (1999) 115–119.
- [5] K. Kümmerer, *J. Antimicrob. Chemother.* 52 (2003) 5–7.
- [6] C.M. Manaia, A. Novo, B. Coelho, O.C. Nunes, *Water, Air, Soil Pollut.* 208 (2010) 335–343.
- [7] N. Sande-Bruinsma, H. Grundmann, D. Verloo, E. Tiemersma, J.M. Goossens, M. Ferech, *Emerg. Infect. Dis.* 14 (2008) 1722–1730.
- [8] K. Torniaainen, J. Mattinen, C.P. Askolin, S. Tammilehto, *J. Pharm. Biomed. Anal.* 15 (1997) 887–894.
- [9] R. Andreozzi, M. Raffaele, P. Nicklas, *Chemosphere* 50 (2003) 1319–1330.
- [10] J.B. Belden, J.D. Maul, M.J. Lydy, *Chemosphere* 66 (2007) 1390–1395.
- [11] E. Fasani, M. Rampi, A. Albini, *Perkin Trans. 2* (1999) 1901–1907.
- [12] K. Torniaainen, E. Mäki, *J. Chromatogr. A* 697 (1995) 397–405.
- [13] M. Mella, E. Fasani, A. Albini, *Helv. Chim. Acta* 84 (2001) 2508–2519.
- [14] T.G. Vasconcelos, D.M. Henriques, A. Köning, A.F. Martins, K. Kümmerer, *Chemosphere* 76 (2009) 487–493.
- [15] J. Burhenne, M. Ludwig, M. Spittler, *Chemosphere* 38 (1999) 1279–1286.
- [16] J. Burhenne, M. Ludwig, P. Nikoloudis, M. Spittler, *Environ. Sci. Pollut. Res.* 4 (1997) 10–15.
- [17] P. Schmitt-Kopplin, J. Burhenne, D. Freitag, M. Spittler, A. Kettrup, *J. Chromatogr. A* 837 (1999) 253–265.
- [18] A. de Juan, E. Casassas, R. Tauler, *Soft-modelling of analytical data*, in: *Encyclopedia of Analytical Chemistry: Instrumentation and Applications*, Wiley, New York, 2000.
- [19] S. Mas, A. de Juan, S. Lacorte, R. Tauler, *Anal. Chim. Acta* 618 (2008) 18–28.
- [20] A. Jayaraman, S. Mas, R. Tauler, A. de Juan, *J. Chromatogr. B* 910 (2012) 138–148.
- [21] C. Fernández, A. De Juan, M.P. Callao, M.S. Larrechi, *Chemom. Intell. Lab. Syst.* 114 (2012) 64–71.
- [22] S. Mas, A. Carbó, S. Lacorte, A. de Juan, R. Tauler, *Talanta* 83 (2011) 1134–1146.
- [23] S. Liu, S. Kokot, G. Will, J. Photochem. Photobiol. C 10 (2009) 152–172.
- [24] M. Garrido, M.S. Larrechi, F.X. Rius, L.A. Mercado, M. Galià, *Anal. Chim. Acta* 583 (2007) 392–401.
- [25] R. Tauler, *Chemom. Intell. Lab. Syst.* 30 (1995) 133.
- [26] R. Tauler, A. Smilde, B.R. Kowalski, *J. Chemom.* 9 (1995) 31.
- [27] A. de Juan, M. Maeder, M. Martínez, R. Tauler, *Chemom. Intell. Lab. Syst.* 54 (2000) 123.
- [28] A. de Juan, M. Maeder, M. Martínez, R. Tauler, *Anal. Chim. Acta* 442 (2001) 337.
- [29] E. Bezemer, S.C. Rutan, *Chemom. Intell. Lab. Syst.* 59 (2001) 19.
- [30] A.R. Carvalho, J. Wattoom, L. Zhu, R.G. Brereton, *Analyst* 131 (2006) 90.
- [31] M. Maeder, A.D. Zuberbülher, *Anal. Chem.* 62 (1990) 2220.
- [32] The Mathworks, *MATLAB Version 7.0*, Natick, MA, 2004.
- [33] R. Tauler, A. Izquierdo-Ridors, E. Casassas, *Chemom. Intell. Lab. Syst.* 18 (1993) 293–300.
- [34] A. Izquierdo-Ridors, J. Saurina, S. Hernández-Cassou, R. Tauler, *Chemom. Intell. Lab. Syst.* 38 (1997) 183–196.
- [35] D.L. Massart, B.G.M. Vandeginste, L.M.C. Buydens, S. de Jong, P.J. Lewi, J. Smeyers-Verbeke, *Handbook of Chemometrics and Qualimetrics: Part A*, Elsevier, Amsterdam, 1997.
- [36] H.R. Keller, D.L. Massart, *Chemom. Intell. Lab. Syst.* 12 (1992) 209.
- [37] M. Amrhein, B. Srinivasan, D. Bonvin, M.M. Schumacher, *Chemom. Intell. Lab. Syst.* 46 (1999) 249–264.
- [38] M. Garrido, I. Lázaro, M.S. Larrechi, F.X. Rius, *Anal. Chim. Acta* 515 (2004) 65–73.
- [39] W. Windig, J. Guilment, *Anal. Chem.* 63 (1991) 1425–1432.
- [40] L.F. Shampine, *Numerical Solutions of Ordinary Differential Equations*, Chapman & Hall, London, 1994.
- [41] L.A. Nelder, R. Mead, *Comput. J.* 7 (1965) 308.
- [42] J. Saurina, S. Hernández-Cassou, R. Tauler, A. Izquierdo-Ridors, *J. Chemometr.* 12 (1998) 183–203.
- [43] A. Lablache-Comber, in: W.M. Horspool, P.S. Song (Eds.), *CRC Handbook of Organic Photochemistry and Photobiology*, CRC Press, Boca Raton, 1995, pp. 1063–1120.
- [44] D.G. Witten, in: O. Buchardt (Ed.), *Photochemistry of Heterocycles*, Wiley, New York, 1976, pp. 524–573.
- [45] A. Albini, S. Monti, *Chem. Soc. Rev.* 32 (2003) 238–250.
- [46] E. Fasani, A. Profumo, A. Albini, *Photochem. Photobiol.* 68 (1998) 666–674.
- [47] M. Sturini, A. Speltini, F. Maraschi, A. Profumo, L. Pretali, E.A. Irastorza, E. Fasani, A. Albini, *Appl. Catal. B Environ.* 119–120 (2012) 32–39.
- [48] E. Fernández, G. Sánchez, *An. R. Acad. Nac. Farm.* 71 (2005) 835–848.
- [49] I.N. Levine, in: *Physical Chemistry*, McGraw-Hill, New York, 2009, pp. 525–526.